Desalination and Water Treatment
www.deswater.com
doi: 10.5004/dwt.2021.26639

212 (2021) 347–358
February

Sorption of anionic and cationic dyes on millet seed envelope from aqueous solution

Abdelkarim Seghier[a,b,*], Rachida Cherrak[b,c], Mohammed Hadjel[b], Nouredine Benderdouche[c]

[a]*University Centre of Relizane Ahmed Zabana, Relizane, BP 48000, Algeria, Tel. +213/542-16-15-12; emails: krimouvert@yahoo.fr/Abdelkarim.seghier@cu-relizane.dz/abdelkarim.seghier@univ-usto.dz (A. Seghier)*
[b]*Laboratory of Sciences, Technologies and Process Engineering, Department of Industrial Organic Chemistry, Faculty of Chemistry, University of Science and Technology – Mohamed BOUDIAF of Oran, BP 1505 El Mnaouar, Bir El Djir 31000 Oran, Algeria, emails: rachidaenv@gmail.com (R. Cherrak), hadjel@yahoo.fr/hadjel100@yahoo.fr (M. Hadjel)*
[c]*Laboratory of Structure, Elaboration and Application of Molecular Materials (SEA2M), University of Abdelhamid Ibn Badis, Mostaganem, Algeria, email: benderdouchen@yahoo.fr*

Received 28 April 2020; Accepted 28 September 2020

ABSTRACT

This study consists of testing the sorption capacity of Methylene blue (MB) and Congo red (CR) on a plant substrate prepared from millet seed envelope (MSE). The solid recovered after each experiment (MSE/MB and MSE/CR) is used as a new adsorbent for second sorption. Fourier transform infrared spectroscopy, scanning electron microscopy coupled with energy dispersive X-ray spectrometer, iodine number, and the point of zero charge determination are used for the characterization of the MSE. The effect of several operating conditions such as contact time, adsorbent dose, pH, initial concentration, and temperature on sorption is investigated. Characterization of the MSE powder showed the presence of several cavities, capillaries, and oxygenated groups distributed over a heterogeneous surface. Energy-dispersive X-ray analysis revealed that aluminum is the most dominant element. The pH_{PZC} value of the sorbent surface is around 6.00. Sorption tests of MB and CR on MSE, MSE/MB, and MSE/CR showed that sorption kinetics is quite fast with an equilibrium contact time of 60 min for the three adsorbents. Sorption kinetics of MB and CR on MSE and MSE recovered is well-described by the pseudo-second-order model. The Langmuir and Freundlich models were found to describe well the sorption of the dyes studied. The determined Langmuir sorption capacities are 111.11 and 94.34 mg/g of MB onto MSE and MSE/CR, respectively, 158.73, and 169.49 mg/g of CR onto MSE and MSE/MB, respectively. The study of the effect of temperature showed that the uptake of MB and CR on MSE is an exothermic process.

Keywords: Adsorption; Millet seed envelope; Acid red; Basic blue; Support recovered

1. Introduction

Environmental pollution has become a socioeconomic problem to be taken into account in a sustainable economy. Water scarcity is a major challenge for many water-stressed countries in the future. However, population growth, industrial development, and agricultural activity negatively impact the sources of drinking water, fauna, and flora, by discharging pollutant-laden waste, which is the cause of several aquatic problems (viruses, heavy metals, and micropollutants, etc.) [1,2]. Synthetic dyes in aqueous effluents are often difficult to treat and biodegrade due to their stable and

* Corresponding author.

complex molecular structure [3]. Methylene blue and Congo red are among the most common dyes present in water discharged from industrial and microbiological and histological activities [4]. According to Juang et al. [5], Methylene blue is responsible for breathing difficulties and its ingestion through the mouth produces a burning sensation; causes nausea, vomiting, sweating, and profuse cold sweats. Albert et al. [6], have shown that Methylene blue causes toxicity in premature neonates. Gillman [7] reported that this dye causes severe toxicity to the central nervous system. Congo red as an Azo dye is considered carcinogenic [8,9]. The Danish Environmental Protection Agency (DEPA, 2000) guidelines for cancer risks assessment established a limited concentration of 3.1 μg/L of azo dye in drinking water [10]. In order to reduce the concentration of these chemicals in water, a wide variety of physical, chemical, and biological techniques have been developed and tested in the treatment of dye-laden effluents [11–36]. However, these procedures are expensive and lead to the generation of large amounts of sludge or the formation of derivatives. Among the liquid discharge treatment processes, adsorption remains a relatively used, and easy to implement technique. The application of the adsorption technique for the treatment of dyes is very old and remains the most widespread technique, given the advantages it has over other techniques. Activated carbon is the most used adsorbent because of its high adsorption capacity of organic materials [37–48]. However, this adsorbent is expensive and difficult to regenerate [38,49,50].

For this reason, several researchers have suggested using low-cost adsorbents for the retention of dyes. For instance, Khan et al. [51], used chir pine sawdust to remove Congo red in batch and column modes. Afroze et al. [52], used raw eucalyptus bark to remove Methylene blue from aqueous solution. Karthik et al. [53], proposed banana fiber, coconut fiber, and sawdust as low-cost adsorbents for Methylene blue removal. The study carried out by Seghier et al. [54] showed that Barbary fig skin can be considered an effective and low-cost biosorbent for the elimination of Congo red. Dutta and Nath [55], synthesized a novel low-cost SiO_2/C nanocomposite from corn cobs for Methylene blue removal.

The present article studies the biosorption of Methylene blue and Congo red on millet seed envelope (MSE) and recovered solid particles after each sorption.

2. Materials and methods

2.1. Raw material and biosorbent preparation

This study consists of preparing a biosorbent from MSE collected from breeders and bird traders in the region of Relizane, Algeria.

The raw material was washed on a column several times with distilled water. The suspension obtained was stirred using a magnetic stirrer for 72 h at a speed of 500 rpm. This operation made it possible to remove all kinds of dust or adhering impurities until clear washing water was obtained. The content was solar dried for 3 d at 38°C. The dried solid was ground into small homogeneous particles. The MSE particles used for adsorption were mechanically separated and the powder with an average diameter of less than 1 mm was kept in a desiccator for subsequent sorption tests. The solids used for the sorption of Methylene blue (MSE/MB) and Congo red (MSE/CR) were recovered, dried, and reused for the removal of Congo red and Methylene blue, respectively.

2.2. Characterization of biomaterial

The knowledge of the physicochemical and structural properties of any material is necessary to contribute to the understanding of many phenomena such as adsorption.

Surface analysis and elementary composition determination of MSE, MSE/MB, and MSE/CR were carried out using a HIROX SH 400 M MEB-EDSBRUKER (Germany) scanning electron microscopy (SEM) coupled with energy dispersive X-ray spectrometer. Iodine number is a determining factor to evaluate the surface area of adsorbents [38,56]. Practically, adsorbents having a good iodine sorption capacity from its aqueous solution have a relatively high specific surface area, suitable for the sorption of organic compounds. The surface area of the MSE was assessed by calculating its iodine value (mg/g) using 100 mL of the standardized iodine solution (0.1 N). The volume was mixed with 1 g of MSE. After equilibrium, the iodine remaining in the supernatants was titrated with a sodium thiosulfate solution (0.1 N). The iodine number is the amount of iodine adsorbed per gram of adsorbent at a residual iodine concentration of 0.02 N [38].

The Fourier transform-infrared (FTIR) spectrum was obtained using a spectrum two FTIR Perkin Elmer (Germany) spectrometer with Universal Attenuated Total Reflectance sampling accessory. The point of zero charge (pH_{PZC}) is the pH at which the surface of the solid has a zero charge. pH_{PZC} of the MSE surface was measured according to the method described by Ferro Garcia [57] where the pH of a NaCl solution (0.01 M) is adjusted between 2 and 12 by adding either hydrochloric acid or sodium hydroxide solution (0.1 N). 0.15 g of the biomaterial was added to each 50 mL vial of NaCl at different pH values. The contents were stirred for 48 h in a thermostatically controlled cell maintained at 25°C. The final pH was measured. The point of intersection between the straight line $pH_f = pH_i$ and the curve obtained corresponds to the pH_{PZC} of the material studied.

2.3. Kinetic sorption study

The experiments were carried out in a very limited field of operating conditions. Their aim is to determine the optimum of the contact time, the support mass, and the pH values so that the equilibrium is almost reached.

2.3.1. Effect of contact time on dyes sorption by MSE and MSE recovered

Twenty-five milliliters of 50 mg/L colored solutions at an initial pH of 6.4 for MB and 7.14 for CR were introduced into series of flasks to which a mass of 0.2 g of MSE and recovered MSE was added. The whole system was stirred at ambient temperature in a thermostatic shaker for time intervals ranging from 0 to 210 min, then the suspensions were centrifuged and the solutions analyzed using a spectrophotometer (SPECORD 200 PLUS – ANALYTIK, JENA,

Germany) at maximum wavelengths of 664 and 495 nm for MB and CR, respectively.

2.3.2. MSE mass effect on MB and CR sorption

Under the same operating conditions (initial concentration of the aqueous solutions, ambient temperature, and initial pH), 25 mL volumes of the MB and CR solutions were contacted with masses ranging from 0.05 to 0.4 g of sorbent and stirred for a contact time determined from the kinetic study. The suspensions were then centrifuged and analyzed at the corresponding wavelength.

2.3.3. pH effect on MB and CR sorption by MSE

The pH of the solution is a key factor to evaluate the effectiveness of the removal of mostly organic substances on adsorbent materials.

The effect of pH was studied in the range of 2.55–10.31 for MB and 6.55–10.04 for CR on 0.2 g of MSE in 25 mL of 50 mg/L colored solution.

The suspensions were stirred at a constant speed. The equilibrium solute concentrations were analyzed after the particles were separated by centrifugation.

2.4. Adsorption isotherms study

Adsorption isotherms play an important role in the determination of the maximum adsorption capacities and in the design of new adsorbents.

The adsorption isotherms for MSE or recovered MSE were studied by using 200 mg of the powdered material in 25 mL of a colored solution at various concentrations. The suspensions were stirred for optimum times of each dye at ambient temperature and then centrifuged and analyzed spectrophotometrically (SPECORD 200 PLUS – ANALYTIK, JENA, Germany).

The same experiments were carried out for temperature values of 25°C, 35°C, and 45°C for MB concentration of 50 mg/L as reported by Aziz et al. [56].

The sorbed amount of Methylene blue and Congo red by the sorbents prepared is expressed by the following formula [55]:

$$q_t = \left(C_0 - C_t\right) \times \frac{V}{m} \tag{1}$$

where q_t is the sorption capacity (mg/g); C_0 and C_e (mg/L) the initial and final adsorbate concentration respectively; V the volume of the aqueous solution (L); m the mass of the sorbent prepared (g).

3. Results and discussion

3.1. Characterization

3.1.1. SEM-EDX interpretation

SEM images at different magnifications show the general structure of the surface of MSE particles with diameters less than 1 mm. The picture shown in Fig. 1c (50 μm enlargement) shows a heterogeneous surface. Micrographs in Figs. 1a and b reveal the presence of several cavities on the external surface and cylindrical capillaries on the internal surface. These observations indicate that the particles of the MSE have an adsorbent surface capable of fixing small organic chemicals such as dyes.

The elemental composition of MSE represented in Table 1 and Fig. 2 shows that aluminum is the most dominant element with a mass percentage exceeding 47%, of which 88.80% is in the combined form Al_2O_3. A significant percentage of oxygen (>45%) reveals the availability of oxygenated sites. We also note the presence of 2.92% by mass of silica, of which 6.25% is in SiO_2 form. No harmful element to the environment in the MSE was detected.

3.1.2. Iodine adsorption capacity

The iodine adsorption capacity of the MSE was found to be 166.92 mg/g. This value indicates that the MSE surface has a good surface area appropriate for uptake of Methylene blue and Congo red for a biosorbent [38].

3.1.3. Point of zero charge pH_{PZC}

The point of intersection between the straight line $pH_f = pH_i$ and the curve obtained is of the order of 6.00 (Fig. 3), the surface is negatively charged for pH higher than pH_{PZC} while it is positively charged for pH < 6.00 [54].

3.1.4. IR spectra analysis

The Fourier transform-infrared (FTIR) spectrum of MSE (Fig. 4) shows the presence of many functions in the surface. Possible spectrum interpretation can be as follows:

At 3,317.14 cm^{-1}, a broadband is assigned to the stretching vibration of the O–H hydroxyl groups of phenols, alcohols, or a carboxylic acid [58,59]. According to Tsamo et al. [60], this vibration can be attributed to the N–H bond of amines. Around 2,917.50 cm^{-1}, a band that generally characterizes the elongation vibrations of the aliphatic C–H bond [54] is observed. The peak recorded at 1,602.33 cm^{-1} accounts for the presence of the aromatic C=C bond (elongation vibration), ketone, aldehyde, or carboxylic acid [61]. The frequency 1,437.07 cm^{-1} is ascribed to the presence of C–H bonds of saturated aliphatic hydrocarbons (alkanes) [61]. The peak recorded at 1,362.92 cm^{-1} is attributed to the elongation vibration of the C–O esters, ether, phenol, or carboxylic bonds [62,63] while at 1,017.28, the peak is due to the elongation of the C–N bonds of the aliphatic amines [64,65].

3.2. Kinetic sorption study

3.2.1. Time effect

The plot of the adsorbed quantity of Methylene blue and Congo red as a function of contact time (Fig. 5) shows that the sorption process is fast. In fact, MB and CR are entirely sorbed by MSE and recovered MSE in the first 30 min of contact time. Thus, after 60 min, equilibrium is reached and the sorption rate is relatively constant with

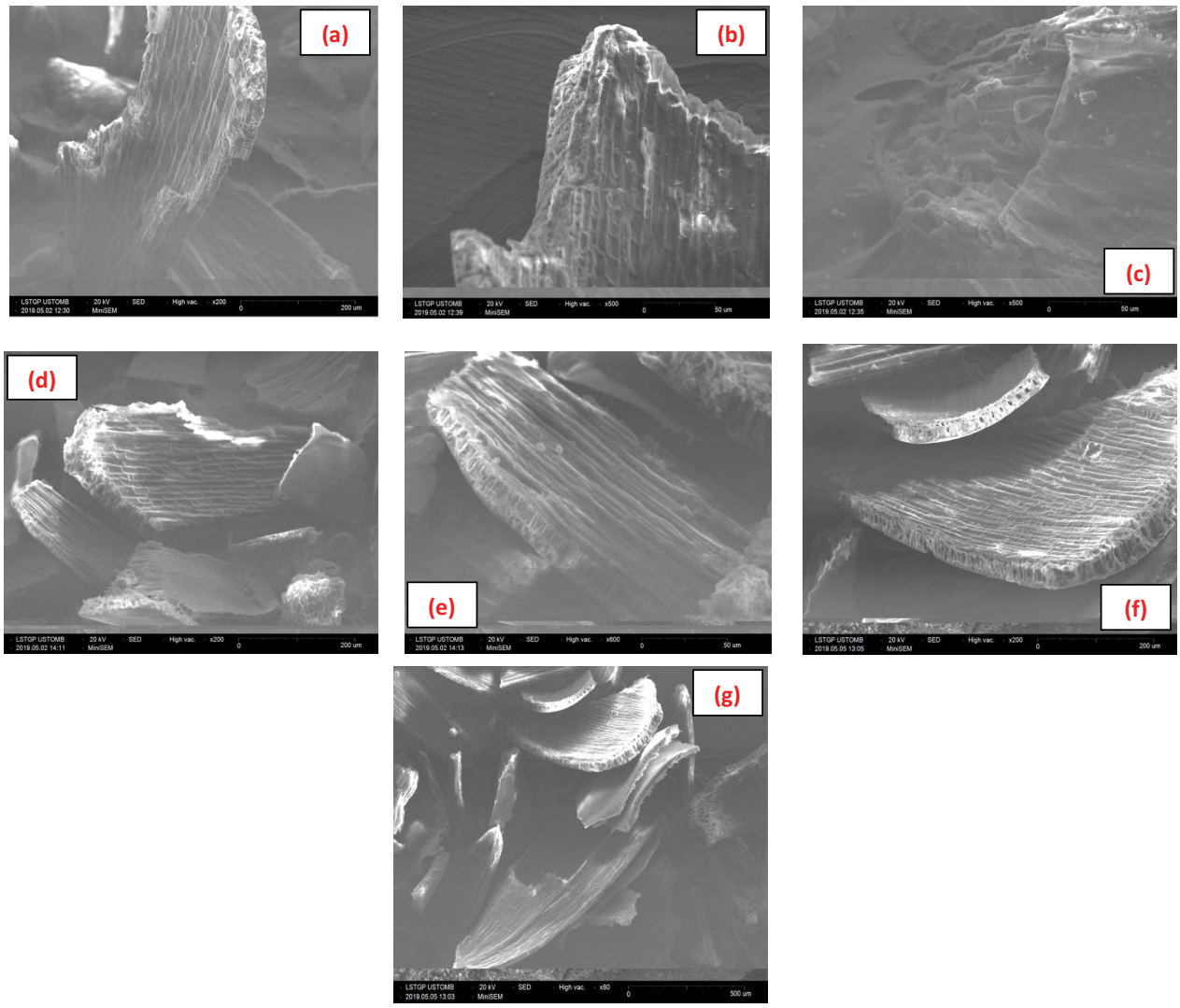

Fig. 1. SEM photographs of the millet seed envelope [(a–c) before sorption (MSE), (d and e) after MB sorption (MSE/MB), and (f and g) after CR sorption (MSE/CR)].

Table 1
Elemental composition of the MSE powder

Element	Norm. C	Atom. C	Compound norm.	Comp. C
	(wt.%)	(at.%)		(wt.%)
Oxygen	45.13	59.91		
Aluminum	47.00	36.99	Al_2O_3	88.80
Silicium	2.92	2.21	SiO_2	6.25
Palladium	0.42	0.08		
Silver	0.48	0.10		

Norm. = Norm.C: the normalised concentration.

elimination capacities of the order of 6.21 and 6.24 mg/g of MB on MSE and MSE/CR, 5.75 and 4.59 mg/g of CR on MSE and MSE/MB, respectively. This rather short time is a good indicator of the availability of sites or adsorbent zones on the surface of the adsorbents used.

3.2.2. MSE mass effect on MB and CR sorption

The percent removal of MB and CR as a function of the MSE dose (Fig. 6) shows that the percent of removal (quantity adsorbed) of the dyes studied increases with

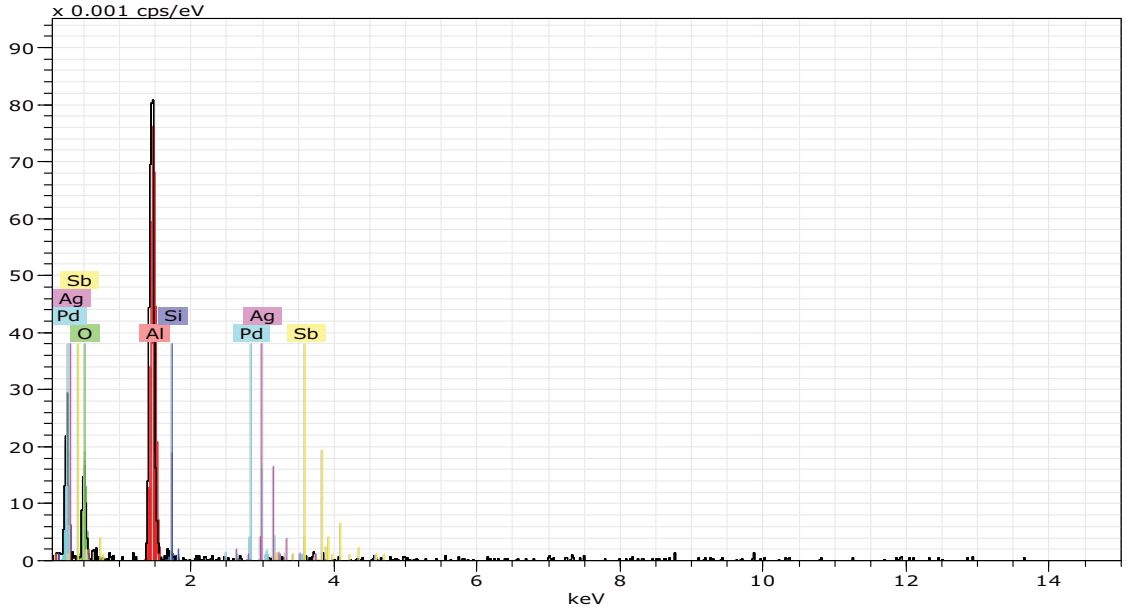

Fig. 2. EDX spectrum of the millet seed envelope surface.

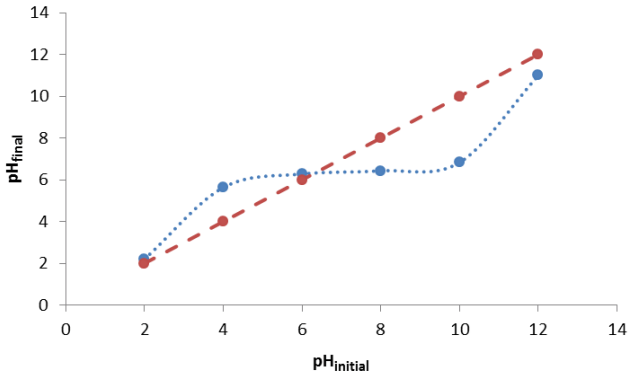

Fig. 3. Representation of the pH_{ZPC} of the surface of MSE.

increasing dose of biosorbent until equilibrium. This is attributed to the increase in the solid/liquid contact surface and the availability of active sites, which promotes the sorption of pollutants on the adsorbent surface [66]. It is noteworthy that the adsorption equilibrium exceeds 98% and 88% for MB and CR with 0.2 g of adsorbent, respectively. From an economic and efficiency point of view, an amount of 0.2 g of MSE is largely sufficient for good removal MB or CR.

3.2.3. pH effect on sorption of MB and CR on MSE

Fig. 7 shows that the best retention rate (99.46%) of Methylene blue on MSE is recorded at a pH value of 6.4. This can be explained on the basis of the zero charge point for the surface biosorbent used. At pH below pH_{ZPC}, a competition of protons with MB for the occupation of the active sites results in a reduction in the amount adsorbed. At pH above this point, the charge on the surface biosorbent becomes negative, which causes greater electrostatic attraction of the basic dye, leading to higher sorption of Methylene blue. When the pH becomes more and more basic, there is a competition between the OH^- ions in the solution and the negative charge of the biosorbent, thus reducing biosorption.

A maximum of 89.49% retention of Congo red was obtained at the neutral pH value. This is explained by the attachment of the CR dye ions to the basic sites (positive charge) of the biosorbent. At a pH below seven, there is a competition between $H3O^+$ and the active sites; on the other hand, at a pH above seven, there is a competition between OH^- and CR ions.

3.2.4. Kinetic mathematical modeling

The order of the reaction is a determining factor in understanding the mechanism of the transfer of sorption of solutes from their aqueous solution to the biosorbent.

The kinetic model of the pseudo-first-order is often formulated by the Lagergren equation [67], which can be expressed as follows:

$$\log\left(q_e - q\right) = \log q_e - \frac{k_1}{2.03} \times t \tag{2}$$

where k_1 (1/min): pseudo-first-order rate constant; t (min): contact time; q_e (mg/g): amount adsorbed at equilibrium at saturation of monolayer; q_t (mg/g): adsorbed quantity (mg/g) per unit mass of the adsorbent at time t.

The pseudo-second-order can be expressed according to the following equation by Ho and McKay [68]:

$$\frac{t}{q_t} = \frac{1}{k_2 q_e^2} + \frac{1}{q_e} \times t \tag{3}$$

where k_2 is the second-order rate constant (g/mg min).

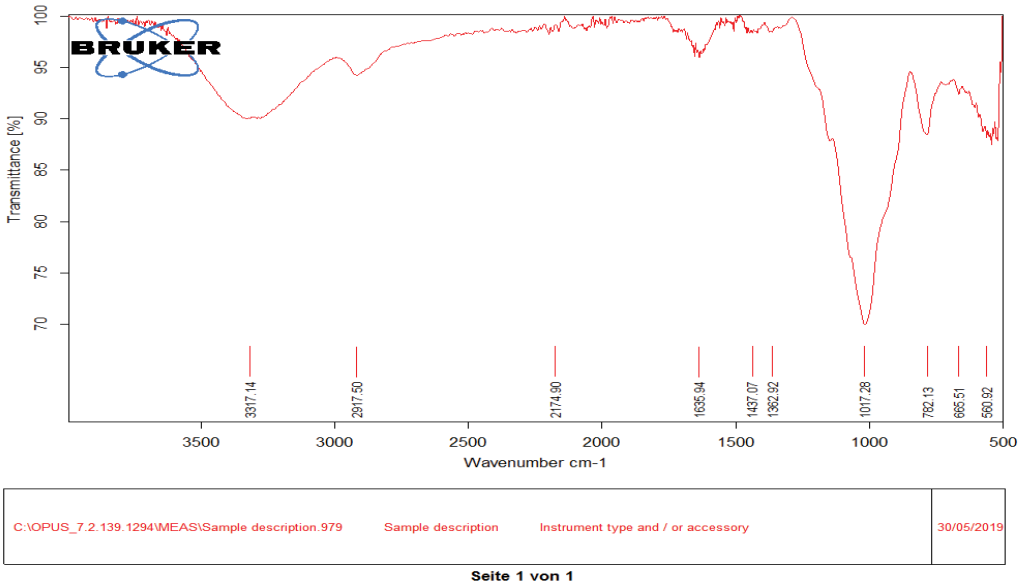

Fig. 4. FTIR spectrum of the millet seed envelope surface.

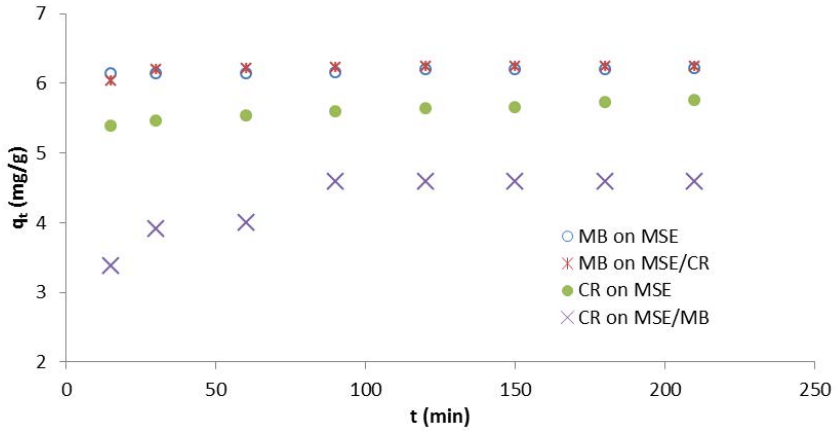

Fig. 5. Time effect on biosorption of MB and CR by MSE and MSE recovered.

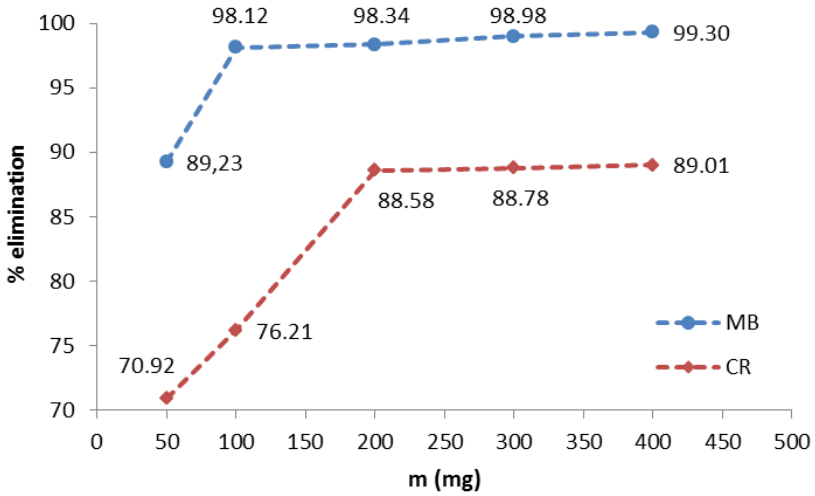

Fig. 6. Effect of MSE dose on biosorption of MB and CR.

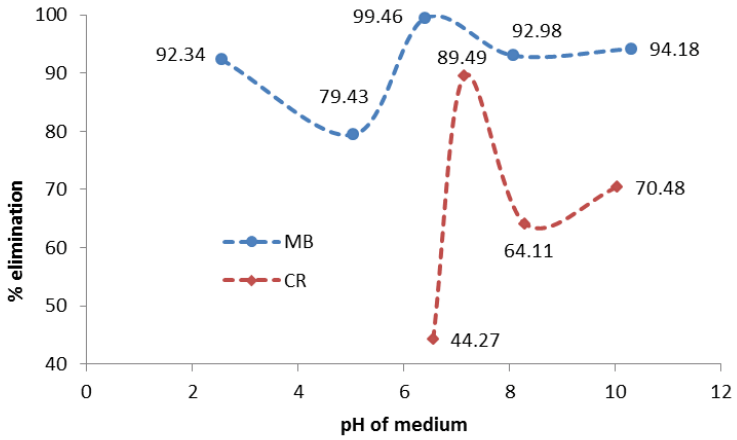

Fig. 7. Effect of the medium pH on the biosorption of MB and CR by MSE.

In order to verify the order of any adsorption kinetics, it is sufficient to graphically display the representative patterns of Eqs. (2) and (3). For the sake of clarity, the kinetic results of all the substances studied are grouped in tabular form in Table 2.

The values of q_{e1} calculated with the pseudo-first-order equation are significantly different from those obtained experimentally, indicating that the data does not obey first-order kinetics. On the contrary, q_{e2} values calculated according to the pseudo-second-order equation are quite close to the experimental results. This reveals a limiting step of the adsorption process, and that the adsorption mechanism is characterized by the mass transfer to the surface of the adsorbent. This conclusion is confirmed by the linearity of the curves of pseudo-second-order equation shown in Fig. 9, with high coefficients of determination R^2 (Table 2). However, the coefficients of determination of the first-order model (Fig. 8) are very low. These observations suggest that chemisorption is the dominant mechanism of the sorption of Methylene blue and Congo red on the materials used [55] by reactions which take place between the functional groups of the surface of the biosorbent and the ions of the basic or acid dye carrying a positive (MB) or negative (CR) charge in aqueous solution, and that the adsorption of MB an CR does not exhibit a controlled diffusion process since it does not follow the pseudo-first-order equation given by Lagergren [69].

3.3. Isotherms sorption study

Increasing the concentration increases the adsorbed amount of solutes from their aqueous solutions until saturation. There are many theoretical models that have been developed to describe adsorption isotherms. However, in this study, we will be particularly interested in the Langmuir and Freundlich models, as they are the simplest and the most widespread.

The Freundlich model is characterized by the following equation [70,71]:

$$\log q_e = \frac{1}{n} \times \log C_e + \log k_F \tag{4}$$

where q_e is the equilibrium adsorbed amount per gram of material (mg/g). C_e represents the equilibrium concentration of the solute in mg/L. k_F and n are the Freundlich constants related to the capacity and intensity of sorption. In addition, the values of n are related to the favorability of the sorption process [72,73].

The mathematical model of Langmuir is expressed by the following equation [70,74]:

$$\frac{C_e}{q_e} = \frac{C_e}{Q_{\max}} + \frac{1}{Q_{\max} \times b} \tag{5}$$

Table 2
Values of the kinetic parameters for the adsorption of MB and CR dyes on different supports

	Solute	MB		CR	
	Sorbent	MSE	MSE/CR	MSE	MSE/MB
	R^2	0.8877	0.9056	0.9094	0.9286
Pseudo-first-order	k_1 (1/min)	0.012	0.021	0.011	0.042
	Calculated q_{e1} (mg/g)	0.121	0.129	0.460	0.313
	Experimental q_e (mg/g)	6.212	6.240	5.752	4.596
	Calculated q_{e2} (mg/g)	6.223	6.254	5.774	4.778
Pseudo-second-order	k_2 (g/mg min)	0.299	0.433	0.080	0.031
	R^2	1	1	0.9998	0.9989

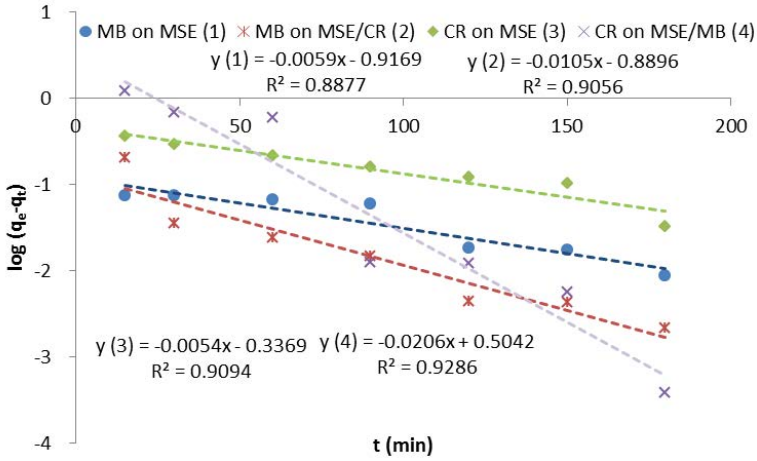

Fig. 8. Kinetic modeling; pseudo-first-order equation of MB and CR biosorption.

where q_e is the equilibrium adsorbed amount per gram of support (mg/g). Q_{max} represents the maximum capacity of the sorption of the solute in mg/g. b (L/mg) is the Langmuir constant corresponding to the adsorption energy.

Moreover, the equilibrium parameter (separation factor) R_L is one of the most important factors discussed in this study, it is calculated by the following relation [54]:

$$R_L = \frac{1}{1 + bC_0} \tag{6}$$

where C_0 (mg/L) is the highest concentration of solute.

The isotherm is unfavorable ($R_L > 1$), linear ($R_L = 1$), favorable ($0 < R_L < 1$), or irreversible ($R_L = 0$).

The exploitation of the formulas in the linear form of Freundlich (Fig. 11) and Langmuir (Fig. 10) allowed us to determine the principal parameters characterizing each model.

Table 3 presents high determination factors for the two models. We can see that the sorption of MB and CR obeys not only the Langmuir model but also the Freundlich model. We also note that the parameters characterizing each adsorption model vary from one medium to another. The values of n between 1 and 10 (Table 3) indicate that the sorption of the two dyes on the various prepared supports is favorable [54].

The calculation of the Langmuir constants (Table 3) shows significant monolayer sorption capacities of 111.11 and 94.34 mg of MB/1 g of MSE and MSE/CR, respectively and of 158.73 and 169.49 mg of CR/1 g of MSE and MSE/MB, respectively. The capacities obtained by this study compare favorably with several materials used in the same field (Table 4).

The values of the Freundlich sorption capacity are 3.81 and 4.45 ($mg^{1-1/n}\ L^{1/n}/g$) of MB onto MSE and MSE/CR, respectively, 3.84 and 3.45 ($mg^{1-1/n}\ L^{1/n}/g$) of CR onto MSE and MSE/MB, respectively. Unlike the Langmuir model, the Freundlich isotherm does not deliver data on the maximum monolayer sorption capacity [75]. However, it gives an idea about the heterogeneous interaction between the ions of the dyes and the adsorbent surface of the biomasses used. Referring to the FTIR analysis surface, functional groups such as carbonyl, carboxyl, phenol, and amine groups may play an important role in this type of interaction [75].

Table 3
Langmuir and Freundlich constants of the sorption of MB and CR by various supports

Pollutants	Adsorbent	Langmuir	Freundlich
MB	MSE	Q_{max} = 111.11 (mg/g)	n = 1.553
		b = 0.015 (L/mg)	K_F = 3.81
		R_L = 0.0008	R^2 = 0.9973
		R^2 = 0.9951	
	MSE/CR	Q_{max} = 94.34 (mg/g)	n = 1.230
		b = 0.033 (L/mg)	K_F = 4.45
		R_L = 0.00015	R^2 = 0.9929
		R^2 = 0.9989	
CR	MSE	Q_{max} = 158.73 (mg/g)	n = 1.223
		b = 0.017 (L/mg)	K_F = 3.84
		R_L = 0.00179	R^2 = 0.9995
		R^2 = 0.9943	
	MSE/MB	Q_{max} = 169.49 (mg/g)	n = 1.328
		b = 0.011 (L/mg)	K_F = 3.45
		R_L = 0.00123	R^2 = 0.9930
		R^2 = 0.9840	

Significant MB and CR sorption capacity values on various adsorbents prepared by this study indicate that MSE, MSE/MB, and MSE/CR can be good low-cost sorbents. R_L values less than 1 indicate that the sorption isotherm is favorable [76]. The good capacity of MB and the amelioration of CR sorption on MSE recovered can be explained by the new more porous structure of the surface of adsorbent materials after MB and CR transfer (Figs. 1d and g).

3.4. Temperature effect on the MB and CR removal on MSE

The results (Fig. 12) indicate that the adsorption capacity of the two substances studied improves with a decrease in temperature. 99.46% and 88.58% removal for MB and CR respectively on MSE are observed at 25°C.

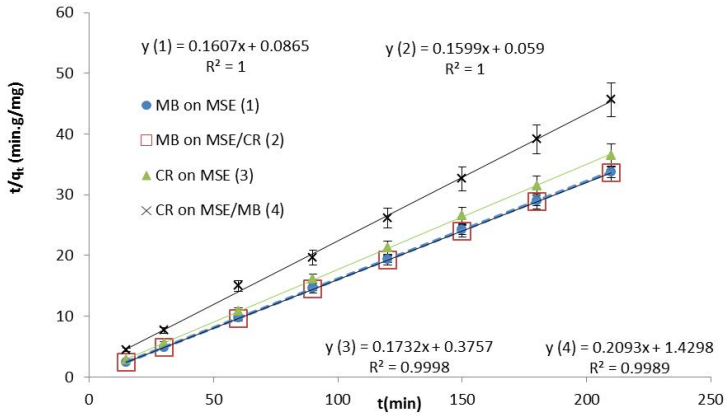

Fig. 9. Kinetic modeling; pseudo-second-order equation of MB and CR biosorption.

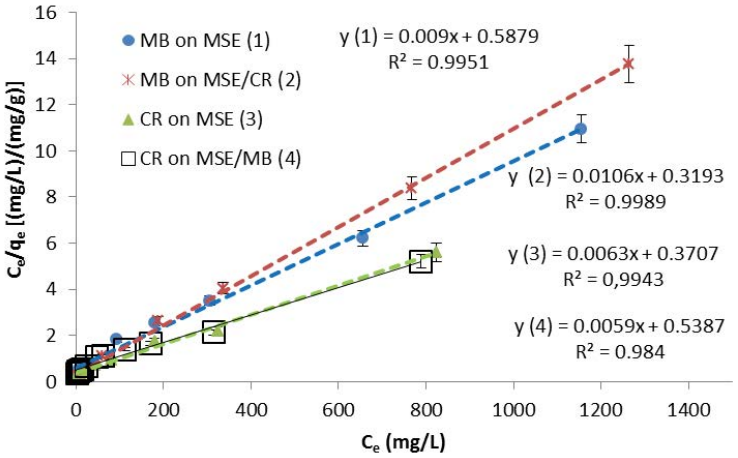

Fig. 10. Isotherm modeling; Langmuir equation of MB and CR biosorption on MSE and MSE recovered.

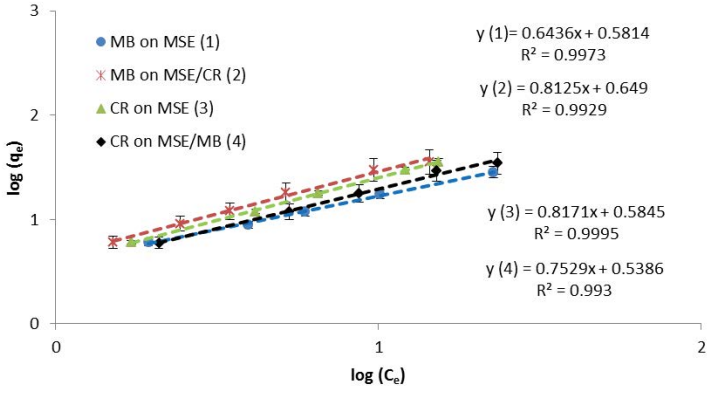

Fig. 11. Isotherm modeling; Freundlich equation of MB and CR biosorption on MSE and MSE recovered.

These findings mean that the dye adsorption process on MSE is exothermic. This may be due to the decrease in the sorption interaction forces between the soluble species and the active sites on the sorbent surface. This phenomenon, in accordance with Arrhenius' law, suggests that the surface reaction is exothermic and that an increase in temperature impairs the sorption process [83].

4. Conclusion

This study aimed at the feasibility of the recovery of a biosorbent for an additional sorption application.

The protocol used for the preparation of the biosorbent and the recovered one shows that it is a low-cost simple procedure that can be applied advantageously.

Table 4
Monolayer Langmuir adsorption capacities in the literatures for MB and CR uptake

	Adsorbent	Q_{max} (mg/g)	Reference
CR	*Alternanthera bettzichiana* plant powder	14.67	[77]
	Activated carbon prepared from choir pith	6.72	[78]
	Ball-milled sugarcane bagasse	38.2	[79]
	Mycelial pellets of Trametesversicolor	51.81	[80]
	MSE	158.73	This study
	MSE/MB	169.49	This study
MB	Brown alga *Cystoseira barbatula* Kützing	38.61	[81]
	Inactivated desert plant	23	[38]
	Pyrolized desert plant	53	[38]
	Plant leaf powder	61.22	[82]
	MSE	111.11	This study
	MSE/CR	94.34	This study

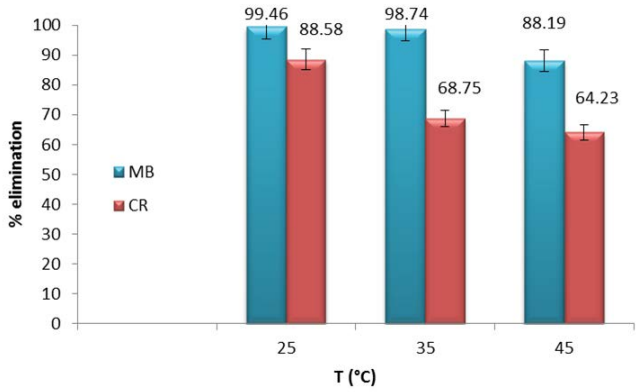

Fig. 12. Temperature effect on the biosorption of MB and CR by MSE.

Characterization of the MSE shows that the sorbent surface has several properties such as the presence of cavities on the external surface, cylindrical capillaries on the internal surface, and oxygenated functional groups.

The sorption kinetics of the solutes on the prepared or recovered MSE shows that the solid/liquid equilibrium contact time is small and that kinetics obeys the pseudo-second-order model. The Freundlich and Langmuir parameters revealed high determination coefficients with high monolayer sorption capacities and solid-solute affinity. The present work shows that the MSE may be a good cost-effective sorbent and that the recovered spent solid may be an efficient new sorbent. Further studies are needed to apply the protocol used in this on an industrial scale.

Acknowledgments

The authors would like to gratefully acknowledge the General Directorate for Scientific Research and Technological Development and the Thematic Agency for Research in Science and Technology, Algeria.

References

[1] R.J. Patrick, Enhancing water security in Saskatchewan, Canada: an opportunity for a water soft path, Water Int., 36 (2011) 748–763.
[2] Y. Wong, Y. Szeto, W. Cheung, G. McKay, Adsorption of acid dyes on chitosan—equilibrium isotherm analyses, Process Biochem., 39 (2004) 695–704.
[3] B. Khalfaoui, A.H. Meniai, R. Borja, Removal of copper from industrial wastewater by raw charcoal obtained from reeds, J. Chem. Technol. Biotechnol., 64 (1995) 153–156.
[4] G.A. Epling, C. Lin, Photoassisted bleaching of dyes utilizing TiO_2 and visible light, Chemosphere, 46 (2002) 561–570.
[5] R. Juang, F. Wu, R. Tseng, The ability of activated clay for the adsorption of dyes from aqueous solutions, Environ. Technol., 18 (1997) 525–531.
[6] M. Albert, M.S. Lessin, B.F. Gilchrist, Methylene blue: dangerous dye for neonates, J. Pediatr. Surg., 38 (2003) 1244–1245.
[7] P.K. Gillman, CNS toxicity involving methylene blue: the exemplar for understanding and predicting drug interactions that precipitate serotonin toxicity, J. Psychopharmacol., 25 (2011) 429–436.
[8] M.A. Brown, S.C. De Vito, Predicting azo dye toxicity, Crit. Rev. Environ. Sci. Technol., 23 (1993) 249–324.
[9] S. Tsuda, N. Matsusaka, H. Madarame, S. Ueno, N. Susa, K. Ishida, N. Kawamura, K. Sekihashi, Y.F. Sasaki, The comet assay in eight mouse organs: results with 24 azo compounds, Mutat. Res., 465 (2000) 11–26.
[10] H. Ben Mansour, O. Boughzala, D. Dridi, D. Barillier, Chekir-Ghedira, L, Mosrati R, Les colorants textiles sources de contamination de l'eau, CRIBLAGE de la toxicité et des méthodes de traitement, J. Water Sci., 24 (2011) 209–238.
[11] C. Du, H. Yang, Z. Wu, X. Ge, G. Cravotto, B.-C. Ye, I. Kaleem, Microwave-assisted preparation of almond shell-based activated carbon for methylene blue adsorption, Green Process. Synth., 5 (2016) 395–406.
[12] L. Kovalova, H. Siegrist, U. Von Gunten, J. Eugster, M. Hagenbuch, A. Wittmer, R. Moser, C.S. McArdell, Elimination of micropollutants during post-treatment of hospital wastewater with powdered activated carbon, ozone, and UV, Environ. Sci. Technol., 47 (2013) 7899–7908.
[13] A.S. Ruhl, F. Zietzschmann, I. Hilbrandt, F. Meinel, J. Altmann, A. Sperlich, M. Jekel, Targeted testing of activated carbons for advanced wastewater treatment, Int. J. Chem. Eng., 257 (2014) 184–190.
[14] A. Aouni, C. Fersi, B. Cuartas-Uribe, A. Bes-Pía, M.I. Alcaina-Miranda, M. Dhahbi, Reactive dyes rejection and textile effluent treatment study using ultrafiltration and nanofiltration processes, Desalination, 297 (2012) 87–96.
[15] Y.K. Ong, F.Y. Li, S.-P. Sun, B.-W. Zhao, C.-Z. Liang, T.-S. Chung, Nanofiltration hollow fiber membranes for textile wastewater treatment: lab-scale and pilot-scale studies, Chem. Eng. Sci., 114 (2014) 51–57.
[16] N. Zaghbani, A. Hafiane, M. Dhahbi, Separation of methylene blue from aqueous solution by micellar enhanced ultrafiltration, Sep. Purif. Technol., 55 (2007) 117–124.

[17] N. Zaghbani, A. Hafiane, M. Dhahbi, Removal of Safranin T from wastewater using micellar enhanced ultrafiltration, Desalination, 222 (2008) 348–356.
[18] L. Zhang, L. Xu, J. He, J. Zhang, Preparation of Ti/SnO_2-Sb electrodes modified by carbon nanotube for anodic oxidation of dye wastewater and combination with nanofiltration, Electrochim. Acta, 117 (2014) 192–201.
[19] V. Khandegar, A.K. Saroha, Electrocoagulation for the treatment of textile industry effluent–a review, J. Environ. Manage., 128 (2013) 949–963.
[20] C.-Z. Liang, S.-P. Sun, F.-Y. Li, Y.-K. Ong, T.-S. Chung, Treatment of highly concentrated wastewater containing multiple synthetic dyes by a combined process of coagulation/flocculation and nanofiltration., J. Membr. Sci., 469 (2014) 306–315.
[21] R. Cherrak, M. Hadjel, N. Benderdouche, S. Bellayer, M. Traisnel, Treatment of recalcitrant organic pollutants in water by heterogeneous catalysis using a mixed material (TiO_2-diatomite of algeria), Desal. Water Treat., 57 (2016) 17139–17148.
[22] V.K. Gupta, R. Jain, A. Mittal, T.A. Saleh, A. Nayak, S. Agarwal, S. Sikarwar, Photo-catalytic degradation of toxic dye amaranth on TiO_2/UV in aqueous suspensions, Mater. Sci. Eng., C, 32 (2012) 12–17.
[23] A. Wang, X. Li, Y. Zhao, W. Wu, J. Chen, H. Meng, Preparation and characterizations of Cu_2O/reduced graphene oxide nanocomposites with high photo-catalytic performances, Powder Technol., 261 (2014) 42–48.
[24] M. Greluk, Z. Hubicki, Kinetics, isotherm and thermodynamic studies of Reactive Black 5 removal by acid acrylic resins, Int. J. Chem. Eng., 162 (2010) 919–926.
[25] S.N. Zhao, X.Z. Song, M. Zhu, X. Meng, L.L. Wu, J. Feng, S.Y. Song, H.J. Zhang, Encapsulation of Ln(III) ions/dyes within a microporous anionic MOF by post-synthetic ionic exchange serving as a Ln(III) ion probe and two-color luminescent sensors, Chem. Eur. J., 21 (2015) 9748–9752.
[26] M. Bilal, M. Asgher, R. Parra-Saldivar, H. Hu, W. Wang, X. Zhang, H.M. Iqbal, Immobilized ligninolytic enzymes: an innovative and environmental responsive technology to tackle dye-based industrial pollutants–a review, Sci Total Environ., 576 (2017) 646–659.
[27] M. Bilal, H.M. Iqbal, H. Hu, W. Wang, X. Zhang, Development of horseradish peroxidase-based cross-linked enzyme aggregates and their environmental exploitation for bioremediation purposes, J. Environ. Manage., 188 (2017) 137–143.
[28] M. Bilal, H.M. Iqbal, H. Hu, W. Wang, X. Zhang, Enhanced bio-catalytic performance and dye degradation potential of chitosan-encapsulated horseradish peroxidase in a packed bed reactor system, Sci. Total Environ., 575 (2017) 1352–1360.
[29] S.A.S. Chatha, M. Asgher, H.M. Iqbal, Enzyme-based solutions for textile processing and dye contaminant biodegradation—a review, Environ. Sci. Pollut. Res., 24 (2017) 14005–14018.
[30] Y. Choi, B. Park, D.K. Cha, Enhancing biological treatment of dye wastewater with zero-valent iron, Korean J. Chem. Eng., 32 (2015) 1812–1817.
[31] A. Ghosh, M.G. Dastidar, T. Sreekrishnan, Biosorption and biodegradation of chromium complex dye using *Aspergillus* species, J. Hazard. Toxic Radioact. Waste, 18 (2014) 1–9.
[32] R. Cherrak, M. Hadjel, N. Benderdouche, M. Adjdir, A. Mokhtar, K. Khaldi, A. Sghier, P.G. Weidler, Preparation of Nano-TiO_2/diatomite composites by non-hydrolytic sol–gel process and its application in photocatalytic degradation of crystal violet, Silicon, 12 (2020) 927–935.
[33] M.N. Khan, O. Bashir, T.A. Khan, S.A. Al-Thabaiti, Z. Khan, CTAB capped synthesis of bio-conjugated silver nanoparticles and their enhanced catalytic activities, J. Mol. Liq., 258 (2018) 133–141.
[34] M.N. Khan, O. Bashir, T.A. Khan, S.A. Al-Thabaiti, Z. Khan, Catalytic activity of cobalt nanoparticles for dye and 4-nitro phenol degradation: a kinetic and mechanistic study, Int. J. Chem. Kinet., 49 (2017) 438–454.
[35] O. Bashir, M.N. Khan, T.A. Khan, Z. Khan, S.A. Al-Thabaiti, Influence of stabilizing agents on the microstructure of Co-nanoparticles for removal of Congo red, Environ. Technol. Innovation, 8 (2017) 327–342.
[36] Z. Khan, O. Bashir, M.N. Khan, T.A. Khan, S.A. Al-Thabaiti, Cationic surfactant assisted morphology of Ag@Cu, and their catalytic reductive degradation of Rhodamine B, J. Mol. Liq., 248 (2017) 1096–1108.
[37] K. Belaroui, A. Seghier, M. Hadjel, Synthesis of activated carbon based on apricot stones for wastewater treatment, Desal. Water Treat., 52 (2014) 1422–1433.
[38] B. Bestani, N. Benderdouche, B. Benstaali, M. Belhakem, A. Addou, Methylene blue and iodine adsorption onto an activated desert plant, Bioresour. Technol., 99 (2008) 8441–8444.
[39] N. Abdel-Ghani, G. El-Chaghaby, E. Zahran, Pentachlorophenol (PCP) adsorption from aqueous solution by activated carbons prepared from corn wastes, Int. J. Environ. Sci. Technol., 12 (2015) 211–222.
[40] J. Li, D.H. Ng, P. Song, C. Kong, Y. Song, P. Yang, Preparation and characterization of high-surface-area activated carbon fibers from silkworm cocoon waste for Congo red adsorption, Biomass Bioenergy, 75 (2015) 189–200.
[41] E. Ekrami, F. Dadashian, M. Arami, Adsorption of methylene blue by waste cotton activated carbon: equilibrium, kinetics, and thermodynamic studies, Desal. Water Treat., 57 (2016) 7098–7108.
[42] L. Ding, B. Zou, W. Gao, Q. Liu, Z. Wang, Y. Guo, X. Wang, Y. Liu, Adsorption of Rhodamine-B from aqueous solution using treated rice husk-based activated carbon, Colloid Surf., A, 446 (2014) 1–7.
[43] R. Han, Y. Wang, W. Yu, W. Zou, J. Shi, H. Liu, Biosorption of methylene blue from aqueous solution by rice husk in a fixed-bed column, J. Hazard. Mater., 141 (2007) 713–718.
[44] A. Mittal, J. Mittal, A. Malviya, D. Kaur, V. Gupta, Adsorption of hazardous dye crystal violet from wastewater by waste materials, J. Colloid Interface Sci., 343 (2010) 463–473.
[45] V. Gupta, A. Mittal, L. Krishnan, V. Gajbe, Adsorption kinetics and column operations for the removal and recovery of malachite green from wastewater using bottom ash, Sep. Purif. Technol., 40 (2004) 87–96.
[46] F. Batzias, D. Sidiras, Dye adsorption by prehydrolysed beech sawdust in batch and fixed-bed systems, Bioresour. Technol., 98 (2007) 1208–1217.
[47] T.A. Khan, E.A. Khan, Shahjahan, Adsorptive uptake of basic dyes from aqueous solution by novel brown linseed deoiled cake activated carbon: equilibrium isotherms and dynamics, J. Environ. Chem. Eng., 4 (2016) 3084–3095.
[48] T.A. Khan, M. Nazir, E.A. Khan, Magnetically modified multiwalled carbon nanotubes for the adsorption of bismarck brown R and Cd(II) from aqueous solution: batch and column studies, Desal. Water Treat., 57 (2016) 19374–19390.
[49] S. Kacha, Z. Derriche, S. Elmaleh, Equilibrium and kinetics of color removal from dye solutions with bentonite and polyaluminum hydroxide, Water Environ. Res., 75 (2003) 15–20.
[50] E. Malkoc, Y. Nuhoglu, Removal of Ni(II) ions from aqueous solutions using waste of tea factory: adsorption on a fixed-bed column, J. Hazard. Mater., 135 (2006) 328–336.
[51] T.A. Khan, S. Sharma, E.A. Khan, A.A. Mukhlif, Removal of Congo red and basic violet 1 by chir pine (*Pinus roxburghii*) sawdust, a saw mill waste: batch and column studies, Toxicol. Environ. Chem., 96 (2014) 555–568.
[52] S. Afroze, T.K. Sen, M. Ang, H. Nishioka, Adsorption of methylene blue dye from aqueous solution by novel biomass *Eucalyptus sheathiana* bark: equilibrium, kinetics, thermodynamics and mechanism, Desal. Water Treat., 57 (2016) 5858–5878.
[53] R. Karthik, R. Muthezhilan, A. Jaffar Hussain, K. Ramalingam, V. Rekha, Effective removal of Methylene Blue dye from water using three different low-cost adsorbents, Desal. Water Treat., 57 (2016) 10626–10631.
[54] A. Seghier, M. Hadjel, N. Benderdouche, Adsorption study of heavy metal and acid dye on an amphoteric biomaterial using barbary fig skin, Arabian J. Sci. Eng., 42 (2017) 1487–1496.
[55] D.P. Dutta, S. Nath, Low cost synthesis of SiO_2/C nanocomposite from corn cobs and its adsorption of uranium(VI), chromium(VI) and cationic dyes from wastewater, J. Mol. Liq., 269 (2018) 140–151.

[56] A. Aziz, M.S. Ouali, E.H. Elandaloussi, L.C. De Menorval, M. Lindheimer, Chemically modified olive stone: a low-cost sorbent for heavy metals and basic dyes removal from aqueous solutions, J. Hazard. Mater., 163 (2009) 441–447.
[57] V. Rives, M.A.A. Ulibarri, Layered double hydroxides (LDH) intercalated with metal coordination compounds and oxometalates, Coord. Chem. Rev., 181 (1999) 61–120.
[58] F. Sakr, A. Sennaoui, M. Elouardi, M. Tamimi, A. Assabbane, Adsorption study of Methylene Blue on biomaterial using cactus, J. Mater. Environ. Sci., 6 (2015) 397–406.
[59] K.F.B. Hossain, M.T. Sikder, M.M. Rahman, M.K. Uddin, M. Kurasaki, Investigation of chromium removal efficacy from tannery effluent by synthesized chitosan from crab shell, Arabian J. Sci. Eng., 42 (2017) 1569–1577.
[60] C. Tsamo, P.D. Djonga, J.D. Dikdim, R. Kamga, Kinetic and equilibrium studies of Cr(VI), Cu(II) and Pb(II) removal from aqueous solution using red mud, a low-cost adsorbent, Arabian J. Sci. Eng., 43 (2018) 2353–2368.
[61] F.Z. Khelaifia, S. Hazourli, S. Nouacer, H. Rahima, M. Ziati, Valorization of raw biomaterial waste-date stones-for Cr(VI) adsorption in aqueous solution: thermodynamics, kinetics and regeneration studies, Int. Biodeterior. Biodegrad., 114 (2016) 76–86.
[62] H. Liu, Q. Gao, P. Dai, J. Zhang, C. Zhang, N. Bao, Preparation and characterization of activated carbon from lotus stalk with guanidine phosphate activation: sorption of Cd(II), J. Anal. Appl. Pyrolysis, 102 (2013) 7–15.
[63] S.L. Knupp, W. Li, O. Paschos, T.M. Murray, J. Snyder, P. Haldar, The effect of experimental parameters on the synthesis of carbon nanotube/nanofiber supported platinum by polyol processing techniques, Carbon, 46 (2008) 1276–1284.
[64] S. Shrestha, G. Son, S.H. Lee, T.G. Lee, Isotherm and thermodynamic studies of Zn(II) adsorption on lignite and coconut shell-based activated carbon fiber, Chemosphere, 92 (2013) 1053–1061.
[65] A. Seghier, M. Hadjel, N. Benderdouche, Comparative study of the sorption capacity and contact time of Congo Red removal in a binary and singular system, Arabian J. Sci. Eng., 43 (2018) 2319–2327.
[66] M. Ghaedi, E. Shojaeipour, A. Ghaedi, R. Sahraei, Isotherm and kinetics study of malachite green adsorption onto copper nanowires loaded on activated carbon: artificial neural network modeling and genetic algorithm optimization, Spectrochim. Acta, Part A, 142 (2015) 135–149.
[67] S.K. Lagergren, About the theory of so-called adsorption of soluble substances, Sven. Vetenskapsakad. Handingarl., 24 (1898) 1–39.
[68] P. Hoet, L. Gilissen, M. Leyva, B. Nemery, *In vitro* cytotoxicity of textile paint components linked to the "Ardystil syndrome", Toxicol. Sci., 52 (1999) 209–216.
[69] K. Belaid, S. Kacha, Étude cinétique et thermodynamique de l'adsorption d'un colorant basique sur la sciure de bois, Water Sci. J., 24 (2011) 131–144.
[70] H. Atout, A. Bouguettoucha, D. Chebli, J. Gatica, H. Vidal, M.P. Yeste, A. Amrane, Integration of adsorption and photocatalytic degradation of methylene blue using TiO_2 supported on granular activated carbon, Arabian J. Sci. Eng., 42 (2017) 1475–1486.
[71] H. Freundlich, Over the adsorption in solution, J. Phys. Chem., 57 (1906) 1100–1107.
[72] S.J. Pollard, C.J. Sollars, R. Perry, A low cost adsorbent from spent bleaching earth. I—the selection of an activation procedure, J. Chem. Technol. Biotechnol., 50 (1991) 265–275.
[73] Y. Yao, F. Xu, M. Chen, Z. Xu, Z. Zhu, Adsorption behavior of methylene blue on carbon nanotubes, Bioresour. Technol., 101 (2010) 3040–3046.
[74] I. Langmuir, The constitution and fundamental properties of solids and liquids. Part I. Solids, J. Am. Chem. Soc., 38 (1916) 2221–2295.
[75] J. Wang, H. Liu, S. Yang, J. Zhang, C. Zhang, H. Wu, Physicochemical characteristics and sorption capacities of heavy metal ions of activated carbons derived by activation with different alkyl phosphate triesters, Appl. Surf. Sci., 316 (2014) 443–450.
[76] K.R. Hall, L.C. Eagleton, A. Acrivos, T. Vermeulen, Pore-and solid-diffusion kinetics in fixed-bed adsorption under constant-pattern conditions, Ind. Eng. Chem., 5 (1966) 212–223.
[77] A. Patil, V. Shrivastava, Alternanthera bettzichiana plant powder as low cost adsorbent for removal of Congo red from aqueous solution, Int. J. ChemTech Res., 2 (2010) 842–850.
[78] C. Namasivayam, D. Kavitha, Removal of Congo Red from water by adsorption onto activated carbon prepared from coir pith, an agricultural solid waste, Dyes Pigm., 54 (2002) 47–58.
[79] Z. Zhang, L. Moghaddam, I.M. O'Hara, W.O. Doherty, Congo Red adsorption by ball-milled sugarcane bagasse, Int. J. Chem. Eng., 178 (2011) 122–128.
[80] A. Binupriya, M. Sathishkumar, K. Swaminathan, C. Kuz, S. Yun, Comparative studies on removal of Congo red by native and modified mycelial pellets of Trametes versicolor in various reactor modes, Bioresour. Technol., 99 (2008) 1080–1088.
[81] D. Caparkaya, L. Cavas, Biosorption of Methylene Blue by a brown alga *Cystoseira barbatula* Kützing, Acta Chim. Slovenica, 55 (2008) 547–553.
[82] V. Gunasekar, V. Ponnusami, Kinetics, equilibrium, and thermodynamic studies on adsorption of methylene blue by carbonized plant leaf powder, J. Chem., 2013 (2013) 415280 6p, doi: 10.1155/2013/415280.
[83] M.A.M. Salleh, D.K. Mahmoud, W.A.W.A. Karim, A. Idris, Cationic and anionic dye adsorption by agricultural solid wastes: a comprehensive review, Desalination, 280 (2011) 1–13.